Mapping Seismic Hazard for Mainland China Using Adaptive Kernel Smoothing Technique

C. Feng[1], H.P. Hong[2]

[1] *Ph.D. Student, Department of Civil and Environmental Engineering, the University of Western Ontario, ON, Canada,*
cfeng43@uwo.ca

[2] *Professor, Department of Civil and Environmental Engineering, the University of Western Ontario, ON, Canada,*
hongh@eng.uwo.ca

Abstract

The information required to develop probabilistic seismic hazard maps includes the seismic source zones, the stochastic earthquake occurrence modeling, and ground motion models. The use of delineated source models and probabilistic seismic hazard assessment is well-known. Other available approaches include the use of a spatially smoothed source model. The present study is focused on the evaluation of probabilistic seismic hazard analysis for mainland China. For the assessment, the adaptive kernel smoothing technique is employed to define the source model by considering the historical seismic catalog, and a set of newly developed ground motion model is applied. Some of the obtained probabilistic seismic hazard maps are compared to the new 5th-generation seismic hazard maps for mainland China, and site-dependent uniform hazard spectra are developed.

Keywords: Probabilistic analysis, seismic hazard, adaptive kernel smoothing, mainland China, uniform hazard spectra.

1. Introduction

The seismic source model, magnitude-recurrence relation, and the ground motion models (GMMs) are the necessary input required for the probabilistic seismic hazard assessment (PSHA). The approach developed by [1] and [2] that is based on the delineated seismic source zones is most frequently used for the PSHA. Other approaches in defining the source models ([3] to [6]) are also considered for PSHA. One of the main differences among these approaches is the degree of spatial smoothing of historical seismicity used to define the seismic source model. The most up to date version (i.e., the 5th-generation) Chinese seismic hazard map (CSHM) is based on the delineated source model [7]. The use of the kernel smoothing approach proposed in [6] was also considered in [8] to estimate the seismic hazard for selected regions in China.

For the development of the 5th-generation CSHM, the GMMs in terms of PGA and PGV were used. These models were developed in [9] (hereafter referred to as YLX13) for Eastern seismic region (ER), Median seismic region (MR), Xinjiang seismic region (XR) and Tibet seismic region (TR) that covering mainland China. The development was based on the projection method [10]. To overcome the lack of applicable GMMs in terms of spectral acceleration (SA), [11] developed the GMMs (BSSA14-P) for mainland China (i.e., a target region) based on the projection method and the GMMs given in [12] (hereafter BSSA14). The use of these GMMs indicates that the design spectrum implemented in Chinses structural design code may be too conservative for structures having long periods.

In the present study, the adaptive kernel smoothing technique is used for the development of the spatially smoothed seismic source models for mainland China, and sets of GMMs that are applicable to regions of China are developed based on projection method and NGA-west2 GMMs ([13] to [20]) (referred to as ASK14, CB14, CY14, and IM14). The developed spatially smoothed seismic source model and the GMMs are used to carry out PSHA for mainland China. The obtained results are compared with those reported in the 5th-generation CSHM.

2. Development of spatially smoothed seismic source models

The historical Chinese earthquake catalog given in [21] and in China earthquake data center (CEDC) (http://data.earthquake.cn/) are considered. The catalog in [21] contains incomplete destructive historical earthquake events that occurred from 1831 BC to 1969 AD. The epicentral locations of the events are shown in Fig 1. Based on cluster analysis, source regions covering mainland China are proposed and also shown in Fig. 1. The model consists of nine seismic regions. The assigned maximum magnitude (M_{smax}) is shown in Fig. 1. The M_{smax} is considered as the maximum of a) the overall maximum magnitude given by Gao et al. (2015) for the seismic source regions and b) the observed maximum magnitude from the historical seismic events plus a tolerance which is set equal to 0.1.

The observation period for the historical earthquake events with different magnitude intervals in the catalog varies. A completeness analysis is carried out using the approach given by [22]. From the analysis, the starting time $T_{C,i}$ for events with M_s greater than $M_{smin,i}$ and occurred before the most present time for the catalog, T_F, is evaluated. This results in the p-th quantile of the period of observation for events with M_s greater than $M_{smin,i}$ $\Delta T_{C,i,p} = T_F - T_{C,i,p}$ to be identified, where $T_{C,i,p}$ denotes the p-th quantile of T_C. The estimated $T_{C,i,p}$ for $p = 0.5$ for the considered nine seismic regions are shown in Fig. 2 for considered $M_{smin,i}$.

Taking into account the obtained $T_{C,i,p}$ for the considered seismic regions, and applying the adaptive procedure ([24] to [27]) the seismicity model is developed. The procedure consists of the following steps:

1) Smooth the occurrence of the j-th seismic event in space using the following kernel function ([6] and [28]),

$$K\left(M_{sj}, s_j, s\right) = \frac{\alpha_1 - 1}{\pi\left[H\left(M_{sj}\right)\right]^2}\left[1 + \frac{\left|s - s_j\right|^2}{\left(H\left(M_{sj}\right)\right)^2}\right]^{-\alpha_1}, \tag{1}$$

where s is a point in space, s_j denote the j-th event with magnitude M_{sj}, $\alpha_1 = 1.8$, and $H\left(M_{sj}\right) = b_1 \exp\left(b_2 M_{sj}\right)$ is the bandwidth function with model parameters b_1 and b_2 that are estimated using the completed catalog [29]. This leads to the pilot estimate of the annual occurrence rate for a site or a cell s_k, $k = 1, \ldots, n_c$, with magnitude greater than M_s, $\lambda_c\left(M_s, s_k\right)$, given by,

$$\lambda_c\left(M_s, s_k\right) = \sum_{j=1}^{n_E} I\left(M_{sj} > M_s\right) \times \frac{1}{\Delta T_j} K\left(M_{sj}, s_j, s_k\right), \tag{2}$$

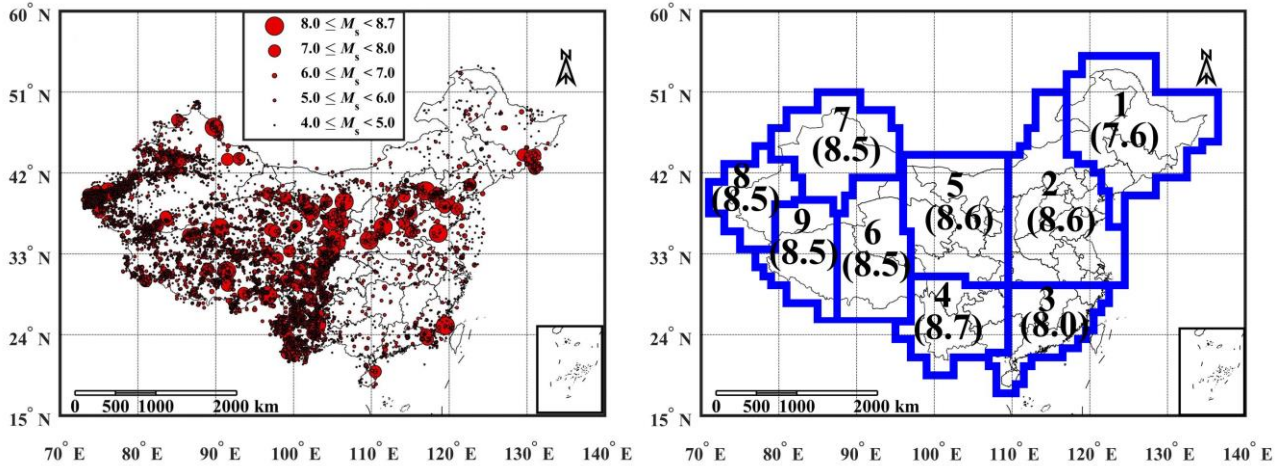where n_E is the total number of events.

Fig. 1 – Left: Epicentral location and M_s of earthquake events in the employed earthquake catalog; Right: nine seismic regions based on cluster analysis from [23]. The maximum magnitude for each seismic region is shown in the bracket.
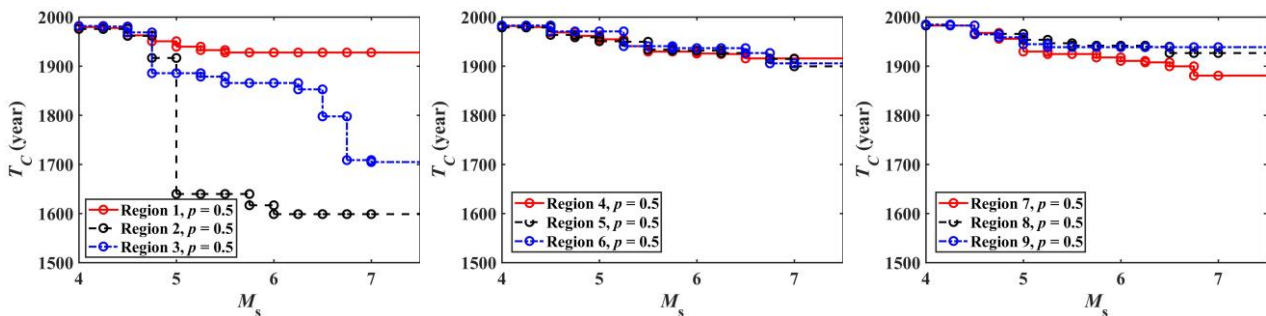

Fig. 2 – Estimated $T_{c,i,p}$ for nine seismic regions for $p = 0.5$ and $M_{smin,i} = M_s$ shown in the horizontal axis.

3

2) Estimate the local bandwidth for a site or a cell s_k, $k = 1, \ldots, n_c$, $c(s_k)$ as a function of M_s,

$$c(M_s, s_k) = \left\{ \left(\prod_{k=1}^{n_c} \lambda_c(M_s, s_k) \right)^{1/n} / \lambda_c(M_s, s_k) \right\}^{\alpha_2}, \tag{3}$$

where α_2 is a model parameter that is considered equal to 0.5 (Silverman 1986).

3) Calculate the rate using the adaptive kernel,

$$\lambda_{c,k}(M_s) = \sum_{j=1}^{n} I\left(M_{sj} > M_s\right) \times \frac{\alpha_1 - 1}{\Delta T_{C,j,p} \times \pi \left[c(s_k) \times H\left(M_{sj}\right) \right]^2} \left[1 + \frac{\left| s_k - s_j \right|^2}{\left(c(s_k) \times H\left(M_{sj}\right) \right)^2} \right]^{-\alpha_1}. \tag{4}$$

Following the above procedure, the $\lambda_{c,k}(4)$ is estimated based on the obtained completed earthquake catalog with $p = 0.5$, for comparison purpose, the $\lambda_{c,k}(4)$ estimated by [23] based on the fixed kernel smoothing is also shown in Fig. 3, it is found that the estimated $\lambda_{c,k}(4)$ based on the two smoothing approaches is similar. The magnitude-recurrence relations based on the smoothed seismic source model given in Fig. 3 for the selected sites are shown in Fig. 4. Again, the magnitude-recurrence relationships obtained based on the fixed kernel smoothing and adaptive kernel smoothing are similar.
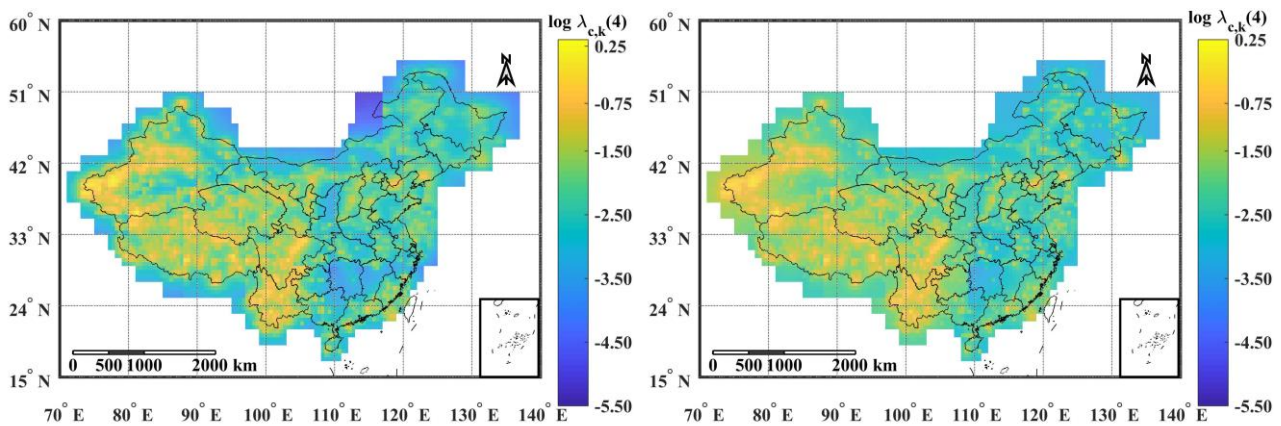

Fig. 3 – Developed spatially smoothed seismic source model based on -Left: using the fixed kernel smoothing approach and -Right: using the adaptive kernel smoothing approach.
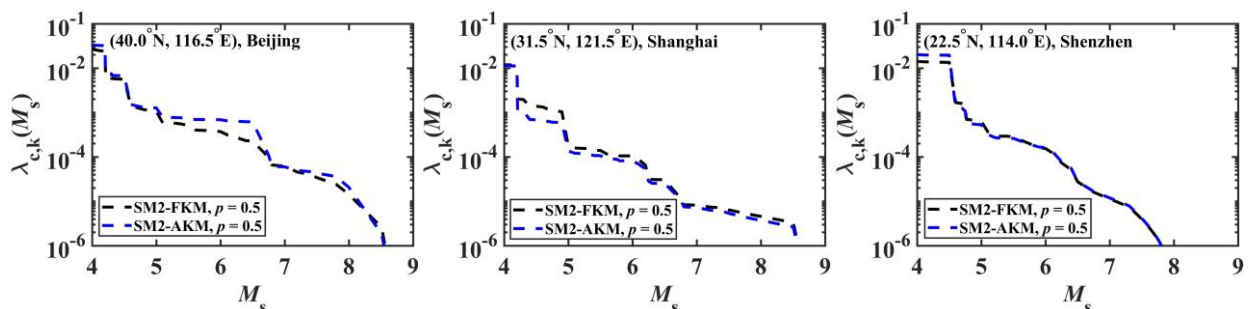

Fig. 4 – Magnitude-recurrence relation based on the fixed kernel smoothing method (FKM) and adaptive kernel smoothing method (AKM).

4

3. Newly developed GMMs employed for seismic hazard mapping

The newly developed GMMs are established based on the projection method [10], the IPEs used in [11], and the GMMs for the reference region, namely ASK14, CB14, CY14, and IM14. The corresponding projected GMMs are referred to as ASK14-P, CB14-P, CY14-P and IM14-P, respectively. These GMMs are given as functions of R_{epi} and M_s. A plot for the developed projected GMMs together with the BSSA14-P and YLX13-G, representing the geometric mean of YLX13, is given in Fig. 5 for reference site class (i.e., Site Class II) [30]. Since YLX13, as well as YLX13-G, are given for Site Class I_1 defined according to [30], a conversion factor for between different site classes suggested in [7] is employed. For comparison purposes, the GMMs considered for the reference region are also shown in the figure.

It is found that the ASK14, BSSA14, CB14, and CY14 are similar for the considered magnitude and distance range, while a relatively larger difference is observed for IM14 with $R_{epi} < 20$km, $M_s = 8$ as compared to ASK14, BSSA14, CB14 and CY14. The median predicted PGA given by YLX13-G is larger than that from the newly projected GMMs for $R_{epi} \leq 100$ km, except for IM14-P, while the trend is reversed for $R_{epi} > 100$ km. $M_s = 5$ and 7 are used for MR because the maximum magnitude applicable for MR is 7 ([7] and [9]).
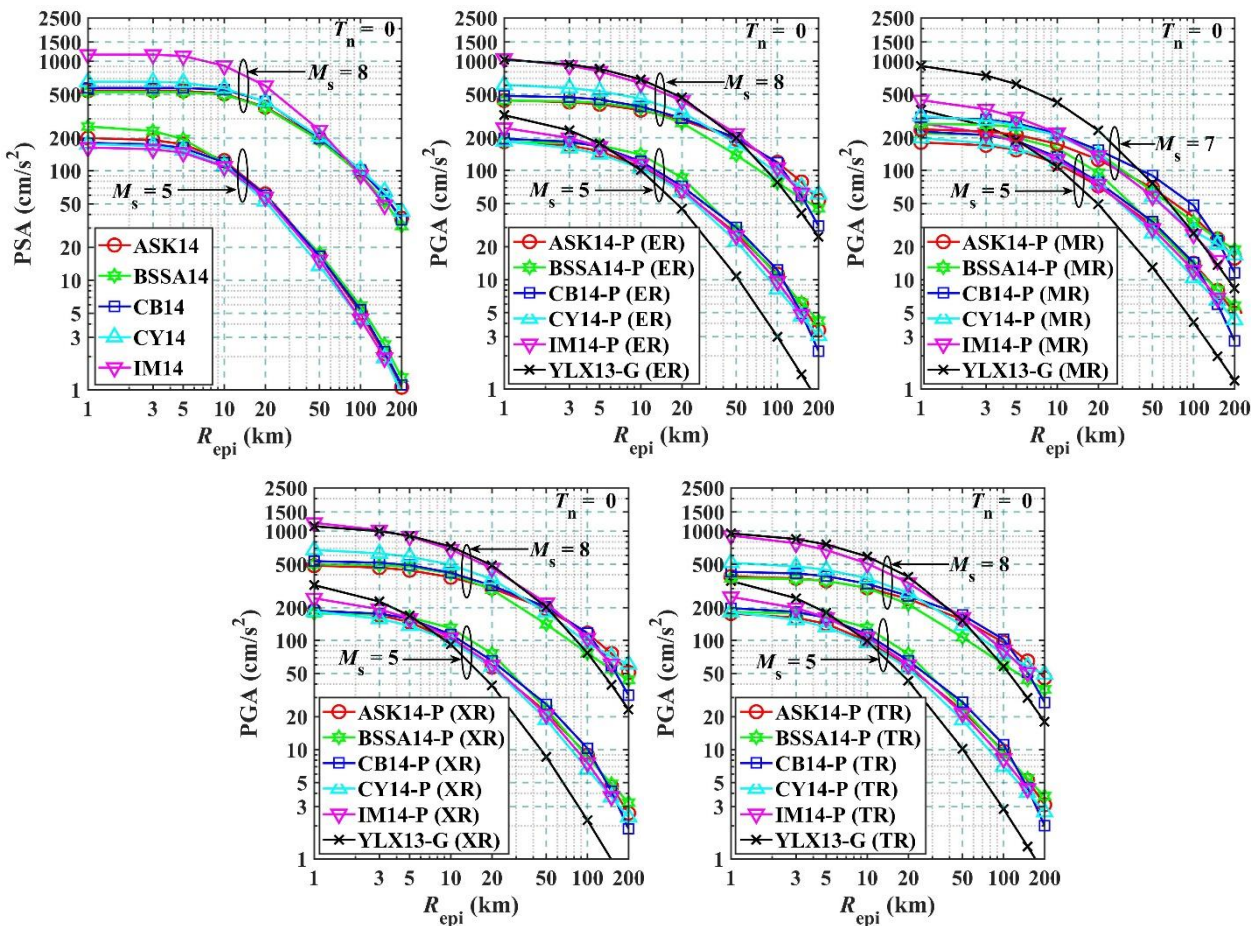

Fig.5 – Comparison for the newly projected GMMs with YLX13 and the NGA-West2 GMMs for Site class II [30].

4. Estimated seismic hazard for selected sites

The seismic hazard for a few chosen sites is estimated by using the spatially smoothed seismic source model

5

that is obtained using the adaptive kernel, and ASK14-P, BSSA14-P, CB14-P, and CY14-P. IM14-P is not used since it is not applicable to a large epicentral distance. The considered GMMs are equally weighted for PSHA. The estimated PGA with 63%, 10%, and 2% exceedance probability in 50 years ($P_E = 63\%$, 10%, and 2%) are listed in Table 1 for site class II [30]. For comparison purposes, the PGA values that are estimated based on the fixed kernel smoothing approach (Feng et al. 2019) and the PGA values for $P_E = 10\%$ that were reported by the 5th-generation CSHM are also included in the table. The table indicates that the estimated seismic hazard is comparable to that given in the 5th-generation CSHM. However, such an agreement is not consistent for all the listed sites in Table 1. In fact, the differences can be as high as 75%. Such a large discrepancy is attributed to the use of different GMMs but most importantly to the seismic source models (i.e., delineated versus spatially smoothed models).

Table 1 – Estimated seismic hazard for the selected sites (FKM = fixed kernel smoothing method, AKM = adaptive kernel smoothing method)

City	(Lat °, Lon °)	Case for $P_E = 63\%$		Case for $P_E = 10\%$			Case for $P_E = 2\%$	
		FKM	AKM	CSHM	FKM	AKM	FKM	AKM
Changchun	(44.0°,125.5°)	0.04	0.04	0.10	0.14	0.13	0.26	0.25
Changsha	(28.0°,112.5°)	0.01	0.02	0.05	0.08	0.08	0.17	0.17
Beijing	(40.0°,116.5°)	0.07	0.08	0.20	0.23	0.25	0.41	0.45
Shanghai	(31.5°,121.5°)	0.04	0.04	0.10	0.15	0.14	0.29	0.28
Shenzhen	(22.5°,114.0°)	0.04	0.05	0.10	0.16	0.19	0.31	0.35
Zhengzhou	(34.5°,113.5°)	0.04	0.04	0.15	0.15	0.15	0.29	0.29
Urumqi	(43.5°,87.5°)	0.15	0.14	0.20	0.35	0.33	0.57	0.54
Yining	(43.5°,81.0°)	0.08	0.08	0.20	0.21	0.21	0.37	0.36
Lhasa	(29.5°,91.0°)	0.11	0.11	0.20	0.29	0.29	0.50	0.51
Tianjin	(39.0°,117.0°)	0.06	0.06	0.20	0.19	0.19	0.35	0.36

The comparison shows that the estimated PGA for $P_E = 63\%$, 10% and 2% for the chosen sites are similar by using the fixed kernel smoothing and adaptive kernel smoothing approaches. The estimated PGA values for $P_E = 10\%$ are comparable to those given by the 5th-generation CHSM. In general, the ratio of 2475-year return period value of PGA to that of 475-year return period value and to that of 50-year return period value varies spatially, with an average about 2 and 6 times, respectively.

The obtained seismic hazard maps in terms of PGA for $P_E = 10\%$ and Site class II are shown in Fig. 6 by adopting the fixed and adaptive kernel soothing techniques. The two spatial trends of the maps presented in the figures are very similar. The obtained normalized UHS for three selected sites with $P_E = 63\%$ 10% and 2% are given in Fig. 7 and are compared with the normalized design spectra given in [30]. It is found that the normalized UHS based on the fixed kernel smoothing and adaptive kernel smoothing approach are almost the same. The value of the normalized UHS is lower than that of the normalized design spectrum for most vibration periods, except for the vibration period within 0.1 and 0.2 s in some cases. This suggests that the normalized design spectrum given in the structural design code [30] may be too conservative.
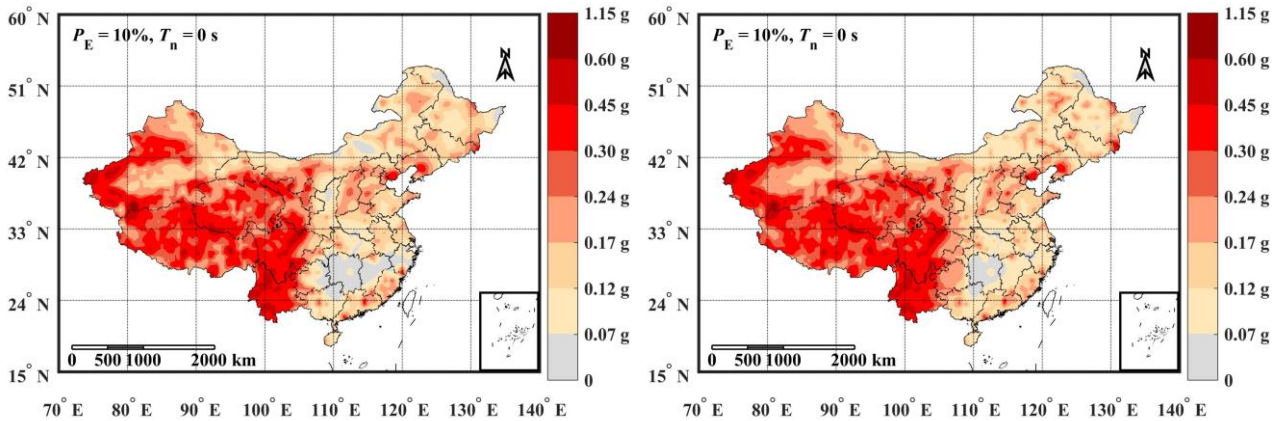
Fig.6 – Seismic hazard map PGA for $P_E = 10\%$: Left: using the fixed kernel smoothing approach and -Right: using the adaptive kernel smoothing approach.
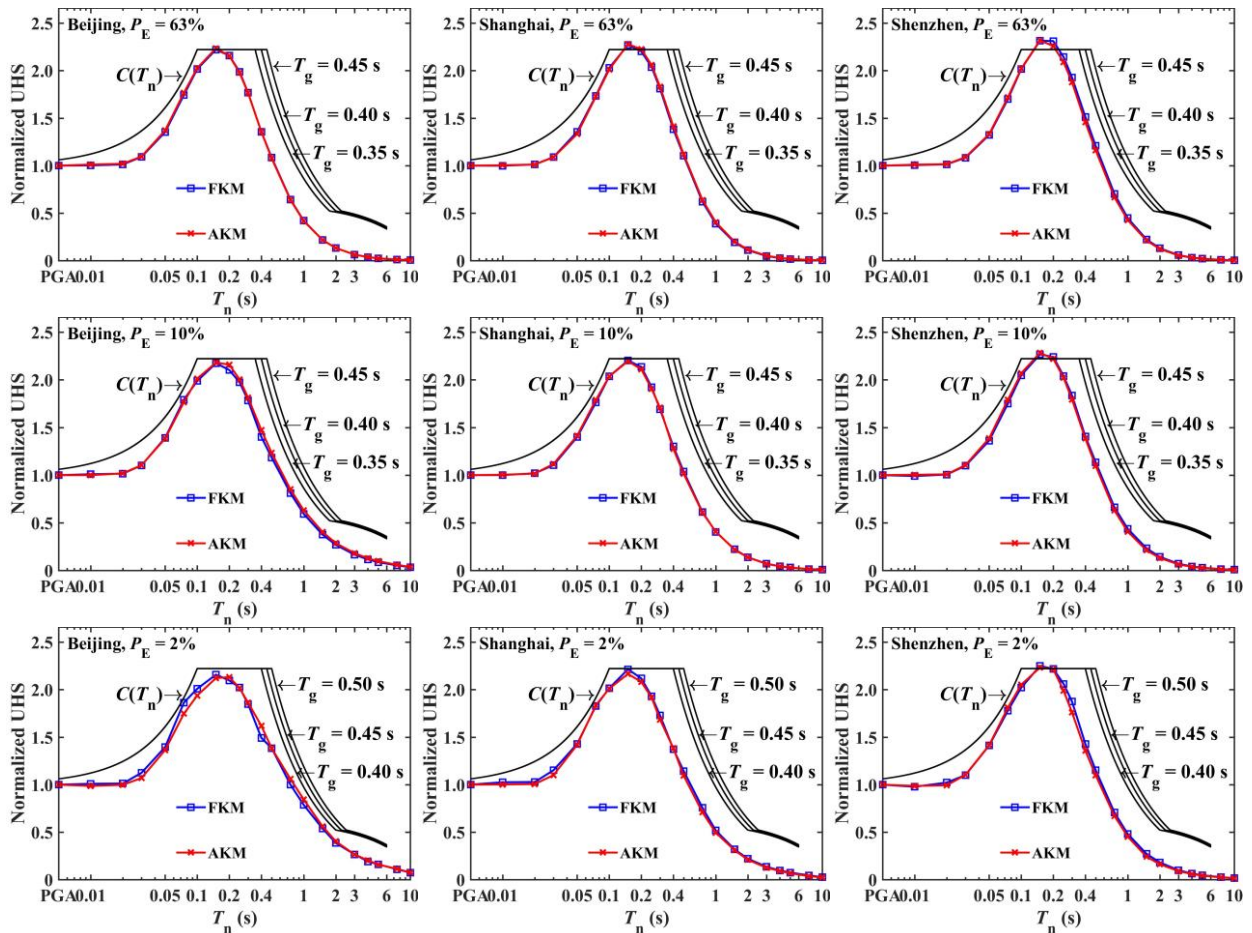

Fig.7 – Normalized UHS for three chosen sites.

3. Conclusions

Completeness analysis is carried out for the historical earthquake catalog of China. The fixed and adaptive kernel smoothing approaches are used to develop the spatially smoothed seismic source models. Using these smoothed seismic source models and a set of newly projected GMMs applicable to regions in China, PSHA is

7

carried out.

For a few chosen sites, the estimated hazard by using the fixed and adaptive kernel smoothing techniques are presented. The estimated values are compared with those reported in the 5th-generation of CSHM. The comparison indicates that the estimated hazard is close to that given by CSHM for some of the chosen sites, while for others, the difference is not negligible. The results also indicate that the use of the fixed or the adaptive kernel smoothing method leads to comparable estimated seismic hazard maps, at least in terms of spatial trends. A comparison between the normalized UHS and normalized design spectrum given in the code indicates that the code suggested normalized design spectrum is conservative, except for structure with the vibration within about 0.1 to 0.2 s. Therefore, a possible improvement could be achieved if the developed UHS is used as a guide to suggest a new design spectrum.

4. Acknowledgments

5. References

[1] Cornell CA (1968): Engineering seismic risk analysis. *Bull. Seism. Soc. Am,* 58 (5), 1583-1606.

[2] Esteva, L (1968): *Bases para la formulación de decisiones de diseño sísmico*. Ph.D's thesis, Instituto de Ingeniería, Universidad Nacional Autónoma de México. (In Spanish)

[3] Milne WG, Davenport AG (1969): Distribution of earthquake risk in Canada. *Bull. Seism. Soc. Am*., Vol. 59 (2), 729-754.

[4] Liu HX (1987): On the seismic zoning map China. *Proceedings of International Seminar on Seismic Zonation*, Guangzhou, China, 35-42. (in Chinese)

[5] Frankel A (1995): Mapping seismic hazard in the central and eastern United State. *Seism. Res. Lett*., 66 (4), 8-21.

[6] Woo G (1996): Kernel estimation methods for seismic hazard area source modeling. *Bull. Seism. Soc. Am*., 86 (2), 353-362.

[7] Gao MT, Li XJ, Xu XW, Wei B, Yu YX, Zhou BG, Zhao FX, Pan H, Lv YJ, Zhou Q, Wu J, Lu DW, Chen K, Li YX, Gao ZW (2015) *GB18306-2015: Introduction to the seismic hazard map of China*. Standards Press of China, Beijing, China. (in Chinese).

[8] Xu WJ, Gao MT (2012): Seismic hazard estimate using spatially smoothed seismicity model as spatial distribution function, *Acta Seismological Sinica*, 34 (4), 525-536 (in Chinese).

[9] Yu YX, Li SY, Xiao L (2013): Development of ground motion attenuation relations for the new seismic hazard map of China. *Technology for earthquake disaster prevention*, 8 (1), 24-33 (in Chinese).

[10] Hu YX, Zhang MZ (1984): A method of predicting ground motion parameters for regions with poor ground motion data. *Earthquake Engineering and Engineering Vibration*, 4 (1), 1-11. (in Chinese)

[11] Hong HP, Feng, C. (2019): On the ground-motion models for Chinese seismic hazard mapping. *Bull. Seism. Soc. Am*. https://doi.org/10.1785/0120180269.

[12] Boore DM, Stewart JP, Seyhan E, Atkinson GM (2014): NGA-west2 Equations for predicting PGA, PGV and 5% Damped PSA for Shallow Crustal Earthquakes, *Earthquake Spectra*. 30 (3), 1057-1085.

[13] Abrahamson NA, Silva WJ, Kamai R (2013): Update of the AS08 ground motion prediction equations based on the NGA-Wet2 data set. *PEER Report No. 2013/04*, Pacific Earthquake Engineering Research Center, University of California, Berkeley.

[14] Abrahamson NA, Silva WJ, Kamai R (2014): Summary of the ASK14 ground motion relation for active crustal regions. *Earthquake Spectra*, 30 (3), 1025-1055.

[15] Campbell KW, Bozorgina Y (2013): NGA-West2 Campbell- Bozorgina ground motion model for the horizontal component of PGA, PGV, and 5%-damped elastic pseudo acceleration response spectra for periods ranging from 0.01 to 10 s. *PEER Report No. 2013/06*, Pacific Earthquake Engineering Research Center, University of California, Berkeley.

[16] Campbell KW, Bozorgina Y (2014): NGA-West2 ground motion model for the average horizontal component of PGA, PGV, and 5%-damped linear acceleration response spectra. *Earthquake Spectra*, 30 (3), 1087-1115.

[17] Chiou BS-J, Youngs R (2013): Update of the Chiou and Youngs NGA ground motion model for average horizontal components of peak ground motion and response spectra. *PEER Report No. 2013/07*, Pacific Earthquake Engineering Research Center, University of California, Berkeley.

[18] Chiou BS-J, Youngs R (2014): Update of the Chiou and Youngs NGA model for the average horizontal components of peak ground motion and response spectra. *Earthquake Spectra*. 30 (3): 1117-1153.

[19] Idriss IM (2013): NGA-West2 model for estimating average horizontal value of pseudo-abosoulte spectral accelerations generated by crustal earthquakes. *PEER Report No. 2013/08*, Pacific Earthquake Engineering Research Center, University of California, Davis.

[20] Idriss IM (2014): An NGA-West2 model empirical model for estimating the horizontal spectral values generated by shallow crustal earthquakes. *Earthquake Spectra*. 30 (3), 1155-1177.

[21] Gu GX, Lin TH, Shi ZL, Li Q, Lu SD, Chen. HT, Wu HY, Yang YL, Wang SY (1983). *Catalog of Chinese Earthquakes 1831 B.C. – 1969 A.D*. Academia Sinica, Scientific Publishing House, Beijing.

[22] Albarello D, Camassi R, Rebez A (2001): Detection of space and time heterogeneity in the completeness of a seismic catalog by a statistical approach: An application to the Italian area. *Bull. Seism. Soc. Am*. 91 (6), 1694-1703.

[23] Feng C, Liu TJ, Hong HP (2019): Seismic hazard assessment for mainland China based on spatially smoothed seismicity. Submitted for publication.

[24] Silverman BW. (1986). *Density Estimation for Statistics and Data Analysis*, Monographs on Statistics and Applied Probability, Chapman and Hall, London

[25] Stock S, Smith EGC CA (2002): Adaptive kernel estimation and continuous probability representation of historical earthquake catalogs. *Bull. Seism. Soc. Am,* 92 (3), 904-912.

[26] Stock S, Smith EGC CA (2002): Comparison of seismicity models generated by different kernel estimations. *Bull. Seism. Soc. Am,* 92 (3), 913-922.

[27] Ramanna CK, Dodagoudar GR (2012): Seismic hazard analysis using the adaptive kernel density estimation technique for Chennai city. *Pure Appl. Geophys*. 169, 55-69.

[28] Vere-Jones D (1992): Statistical methods for the Description and Display of Earthquake Catalogs. *Statistics in Environmental and Earth Sciences*, Edward Arnold, London, 220-246.

[29] Goda K, Aspinall W, Taylor CA (2013): Seismic hazard analysis for the UK: Sensitivity to spatial seismicity modelling and ground motion prediction equations. *Seism. Res. Lett*., 84 (1), 112-129.

[30] GB50011-2010. (2010): *Code for seismic design of buildings*, Ministry of Housing and Urban-Rural Development of the People's Republic of China (MOHURD), Beijing, China.